ETH zürich

ETH Library

Injury Signals Cooperate with Nf1 Loss to Relieve the Tumor-Suppressive Environment of Adult Peripheral Nerve

Journal Article

Author(s):
Ribeiro, Sara; Napoli, Ilaria; White, Ian J.; Parrinello, Simona; Flanagan, Adrienne M.; Suter, Ueli; Parada, Luis F.; Lloyd, Alison C.

Publication date:
2013-10

Permanent link:
https://doi.org/10.3929/ethz-b-000072083

Rights / license:
Creative Commons Attribution-NonCommercial-NoDerivs 3.0 Unported

Originally published in:
Cell Reports 5(1), https://doi.org/10.1016/j.celrep.2013.08.033

This page was generated automatically upon download from the ETH Zurich Research Collection.
For more information, please consult the Terms of use.

Cell Reports
Article

Injury Signals Cooperate with *Nf1* Loss to Relieve the Tumor-Suppressive Environment of Adult Peripheral Nerve

Sara Ribeiro,[1,2] Ilaria Napoli,[1,2] Ian J. White,[1] Simona Parrinello,[1,2] Adrienne M. Flanagan,[2,3] Ueli Suter,[4] Luis F. Parada,[5] and Alison C. Lloyd[1,2,*]
[1]MRC Laboratory for Molecular Cell Biology, University College London, Gower Street, London WC1E 6BT, UK
[2]UCL Cancer Institute, University College London, Gower Street, London WC1E 6BT, UK
[3]Histopathology Department, Royal National Orthopaedic Hospital NHS Trust, Middlesex HA7 4LP, UK
[4]Department of Biology, Institute of Molecular Health Sciences, ETH, 8093 Zurich, Switzerland
[5]Department of Developmental Biology and Kent Waldrep Foundation Center for Basic Research on Nerve Growth and Regeneration, University of Texas Southwestern Medical Center, Dallas, TX 75390, USA
*Correspondence: alison.lloyd@ucl.ac.uk
http://dx.doi.org/10.1016/j.celrep.2013.08.033
This is an open-access article distributed under the terms of the Creative Commons Attribution-NonCommercial-No Derivative Works License, which permits non-commercial use, distribution, and reproduction in any medium, provided the original author and source are credited.

SUMMARY

Schwann cells are highly plastic cells that dedifferentiate to a progenitor-like state following injury. However, deregulation of this plasticity, may be involved in the formation of neurofibromas, mixed-cell tumors of Schwann cell (SC) origin that arise upon loss of NF1. Here, we show that adult myelinating SCs (mSCs) are refractory to Nf1 loss. However, in the context of injury, Nf1-deficient cells display opposing behaviors along the wounded nerve; distal to the injury, $Nf1^{-/-}$ mSCs redifferentiate normally, whereas at the wound site $Nf1^{-/-}$ mSCs give rise to neurofibromas in both $Nf1^{+/+}$ and $Nf1^{+/-}$ backgrounds. Tracing experiments showed that distinct cell types within the tumor derive from Nf1-deficient SCs. This model of neurofibroma formation demonstrates that neurofibromas can originate from adult SCs and that the nerve environment can switch from tumor suppressive to tumor promoting at a site of injury. These findings have implications for both the characterization and treatment of neurofibromas.

INTRODUCTION

Neurofibromatosis type 1 (NF1) is a common autosomal-dominant inherited disease that affects one in 3,500 people worldwide. The hallmark of this disease is the development of neurofibromas—heterogeneous, benign tumors composed of a mixture of Schwann cells (SCs), axons, ''perineurial-like'' cells, inflammatory cells, and vascular cells embedded in a rich extracellular matrix. Neurofibromas can be classified as dermal (arising exclusively in the skin) or plexiform (developing along the nerve plexus). Although dermal and plexiform neurofibromas are similar at the cellular and ultrastructural levels, only the latter can progress to the highly malignant tumors known as malignant peripheral nerve sheath tumors (MPNSTs) (Ferner, 2007; Riccardi, 1992). Despite their mixed-cell composition, neurofibromas have been shown to originate from SCs (the main type of glia in the peripheral nervous system [PNS]) that have undergone biallelic loss of *NF1*. *NF1* codes for neurofibromin, a Ras-GTPase activating protein (Ras-GAP) that negatively regulates Ras signaling by accelerating the conversion of active Ras-GTP to inactive Ras-GDP (Martin et al., 1990; Xu et al., 1990). Loss of neurofibromin leads to hyperactivation of Ras and its downstream effectors, and accordingly, elevated levels of Ras signaling are detected in $NF1^{-/-}$ SCs isolated from neurofibromas or MPNSTs and have been shown to be critical for the maintenance of a transformed phenotype (Basu et al., 1992; DeClue et al., 1992; Kim et al., 1997).

In the adult, SCs exist in one of two highly quiescent, specialized states: myelinating SCs (mSCs), which myelinate larger axons, or non-mSCs, which bundle together groups of smaller axons in structures known as Remak bundles (Jessen and Mirsky, 2005). There is no identified stem cell population in the nerve to produce new cells; instead, differentiated SCs have the capacity to dedifferentiate to a progenitor-like state. This plasticity of SCs is critical for the ability of the PNS to regenerate. Traumatic injury to the PNS produces acute tissue damage at the lesion site. Distal to the wound site, the nerve stump undergoes a series of well-characterized molecular and cellular events known as Wallerian degeneration (WD). During WD, axons downstream of the injury site degenerate, leaving behind SCs that dedifferentiate to a progenitor-like state and divide inside their basal lamina. The dedifferentiated SCs, together with resident and infiltrating macrophages, clear the axonal and myelin debris, thereby generating a conducive environment for newly formed axons. The SCs then organize themselves into cellular cords that will guide the regrowing axons back to their targets. This period is associated with a robust inflammatory response: inflammatory cells, including mast cells, neutrophils, and T cells, enter the nerve in large numbers, both at the damage

site and throughout the length of the distal stump. Following axonal regrowth, SCs redifferentiate in response to axonal signals and the inflammatory response resolves to give rise to a repaired and functional nerve (Fawcett and Keynes, 1990; Scherer and Salzer, 2001; Zochodne, 2008). It has frequently been observed that neurofibromas resemble the "injured" state in that they are composed of a similar complex mixture of cells found in the nerve following injury, and the SCs in the tumor are dedifferentiated and mostly dissociated from axons. Because of this, neurofibromas have been referred to as "unrepaired wounds" (Parrinello and Lloyd, 2009; Riccardi, 1992).

Recent work from our laboratory has shown that strong and sustained activation of the Raf/ERK Ras-downstream pathway in SCs in vivo is sufficient to induce fully differentiated mSCs to revert to a progenitor-like state and dissociate from axons (Napoli et al., 2012; Parrinello et al., 2008). Moreover, we found that signals from the dedifferentiated SCs orchestrated the inflammatory response via the secretion of cytokines. Therefore, a reasonable model of neurofibroma formation suggested that *NF1* loss via elevated Ras/Raf/ERK signaling would be sufficient to drive many of the early stages of tumor formation.

However, recent mouse models have contradicted this simple model. Loss of *Nf1* in SCs during development resulted in the formation of normal nerves, although tumors developed in adulthood, whereas loss of *Nf1* in adult SCs did not result in frequent tumor formation (Joseph et al., 2008; Le et al., 2011; Wu et al., 2008; Zheng et al., 2008). These results suggested that in the context of the nerve, *Nf1* loss does not affect the ability of SCs to interact with axons or differentiate, and indicated that *Nf1* needed to be lost at a specific stage during development to "prime" the SC for later tumor development triggered by rare later events (Parrinello and Lloyd, 2009). Moreover, other cell types also appeared to be important for the development of neurofibromas, as tumors frequently developed only in a $Nf1^{+/-}$ background, suggesting that other $Nf1^{+/-}$ cell types are required for tumor formation (Yang et al., 2008; Zhu et al., 2002).

Here, we analyzed the effect of *Nf1* loss in adult mSCs. We found that *Nf1* loss was unable to induce ERK activation in adult mSCs, had no effect on the structure of the nerve, and did not result in tumors. However, we found that following injury, *Nf1*-deficient mSCs formed neurofibromas specifically at the wound site. Interestingly, these tumors formed with a similarly high frequency in both $Nf1^{+/-}$ and $Nf1^{+/+}$ backgrounds. These results show that adult mSCs can be the "cell of origin" for neurofibromas. Moreover, they demonstrate that the tumor-suppressive environment of the nerve can be converted to a tumor-promoting environment at a wound site that cooperates with $Nf1^{-/-}$ SCs to form a neurofibroma. They also identify an alternative mouse model for neurofibroma formation that should be useful for studying the early stages of tumor formation and identifying novel therapeutic strategies.

RESULTS

Targeting Loss of *Nf1* in Adult mSCs

To test the effects of *Nf1* loss in adult mSCs, we selected a conditional transgenic mouse line expressing the tamoxifen (Tmx)-inducible Cre recombinase (Cre-ERT2) under the control of an SC-specific promoter, P0, which has been shown to be highly specific for mSCs (Leone et al., 2003; Messing et al., 1992, 1994). To confirm the specificity of Cre-ERT2 expression and determine the efficiency of recombination, we initially crossed the P0-CreER mice to Rosa26-YFP reporter mice (*P0:YFP*). The progeny were treated with Tmx for 5 consecutive days and 15 days later, sciatic nerve cryosections were immunostained for yellow fluorescent protein (YFP) and either the mSC marker, P0, or the non-mSC marker, p75. As shown in Figures 1A and 1B, the specificity of recombination appeared to be highly specific for mSCs, as the only detectable YFP+ cells within the sciatic nerve were also P0+. This specificity was confirmed in multiple nerves and sections in which we failed to find a single p75+/YFP+ cell (Figure 1B) or a single YFP+/P0− cell, confirming that recombination was not only restricted to SCs but also confined to mSCs. The efficiency of recombination, as determined by counting the percentage of P0+ cells that were positive for YFP, was variable between animals, ranging from a minimum of 15% to a maximum of approximately 50% (Figure 1C). Next, *P0-CreER* mice were mated with $Nf1^{fl/fl}$ (Zhu et al., 2001) and $Nf1^{fl/-}$ (Brannan et al., 1994) mice to generate both *P0-*$Nf1^{fl/fl}$ and *P0-*$Nf1^{fl/-}$ mice. $Nf1^{fl/fl}$ and $Nf1^{fl/-}$ mice were used as controls, as a $Nf1^{+/-}$ genetic background has been shown to be critical for tumor formation in some NF1 mouse tumor models (Le and Parada, 2007; Zhu et al., 2002). Two weeks following Tmx treatment, recombination was confirmed by PCR (not shown) and neurofibromin expression was analyzed by western blot, which showed a significant loss of neurofibromin expression in the *P0-*$Nf1^{fl/fl}$ and *P0-*$Nf1^{fl/-}$ mice (Figure 1D).

Loss of *Nf1* in Adult mSCs Fails to Activate ERK Signaling or Stimulate Proliferation

To determine the effects of *Nf1* loss in adult mSCs, we initially analyzed the sciatic nerves 15 days after the first Tmx injection. We analyzed the number of p75+ cells, which as a marker of dedifferentiated SCs would indicate that SC dedifferentiation had taken place, and performed an analysis of 5-ethynyl-2′-deoxyuridine (EdU) incorporation to detect aberrant proliferation (Figure 1A and S1A). In both cases, we were unable to detect differences between controls and *Nf1* mutants, indicating that *Nf1* loss does not induce a rapid induction of SC dedifferentiation and/or proliferation (Figures 2A and S1A). To determine whether *Nf1* loss in adult SCs led to changes in the structure of the nerves over the longer term, as was seen in mice in which *Nf1* was knocked out in SCs during development, we analyzed the structure of the nerves at 8 months following *Nf1* deletion. Analysis of semithin sections of the sciatic nerves showed no detectable differences in the structure of myelinated axons between *Nf1* mutants and controls (Figure 2B). Moreover, ultrastructural analysis of mutant and control animals revealed normal Remak bundles (Figure S1B), which were the first indicators of the initiation of hyperplasia in other NF1 model mice (Wu et al., 2008; Zheng et al., 2008), and the lack of an inflammatory response (Figures S1C and S1D). Furthermore, no tumors were observed in >60 animals for up to 15 months following the Tmx injections. Consistent with the lack of any phenotype, we could not detect any alteration of ERK activation in *Nf1* mutants either by western blot analysis of sciatic nerve lysates (Figure 2C) or by

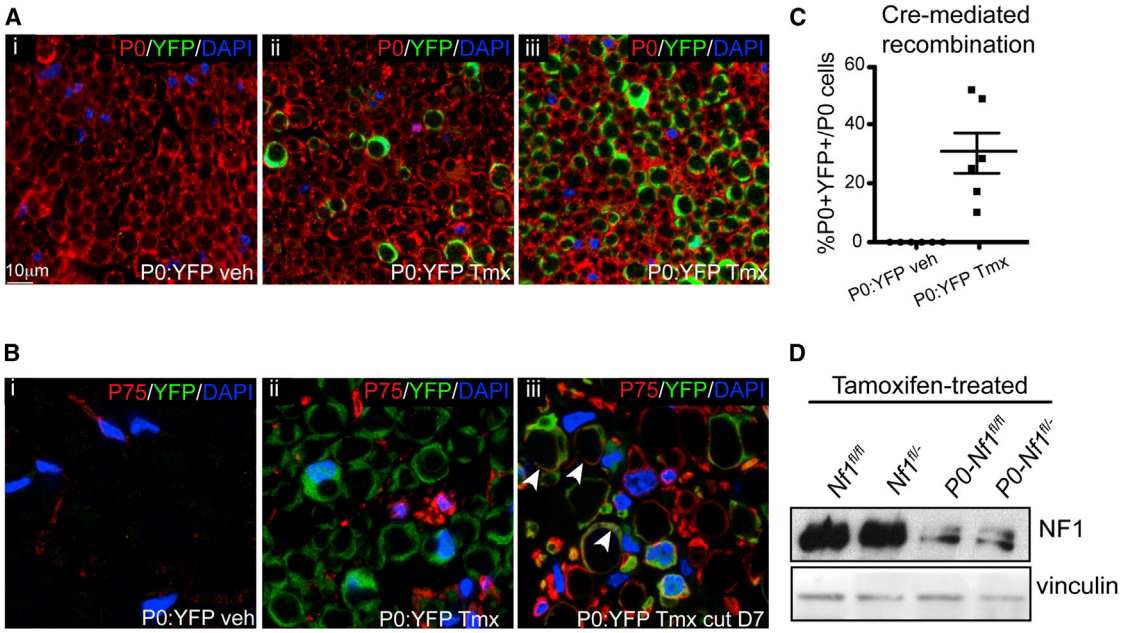

Figure 1. P0;Cre-Recombinase Activity Specific to mSCs Induces Neurofibromin Loss

(A) Sciatic nerve cryosections of *P0:YFP* mice following vehicle (i) or Tmx treatment (ii and iii) were labeled with DAPI, P0, and YFP antibody to identify Cre+ mSCs.

(B) Cryosections of Tmx-treated *P0:YFP* animals were labeled for YFP and the nonmyelinating/dedifferentiated SC marker p75. No colocalization was found in intact nerves (i and ii). As a positive control, iii shows an injured nerve from Tmx-treated mice in which dedifferentiating YFP+ cells were found to colocalize with p75 staining (white arrowheads) 7 days after nerve transection.

(C) Graphs show quantification of the percentage of P0+/YFP+ cells (n = 6 animals for each group; ten different fields were counted for each section, and three sections were counted for each animal; graphs show mean values ± SEM).

(D) Western blot analysis of neurofibromin expression in mouse sciatic nerve lysates 15 days after Tmx administration.

immunofluorescence of sciatic nerve sections (Figure 2D). Therefore, *Nf1* deletion in adult mSCs is not sufficient to activate Ras/ERK signaling or induce a phenotypic or tumorigenic response.

Neurofibromas Develop Specifically at a Wound Site

In mice in which *Nf1* is knocked out during development, the nerves develop normally. However, as the mice age, the structures of the nerves show abnormalities, with SCs dissociating from axons, and the mice eventually develop tumors, indicating that additional, possibly environmental, signals are involved (Wu et al., 2008; Zheng et al., 2008). We decided to test whether wounding of the sciatic nerve might cooperate with loss of *Nf1* to induce tumorigenesis, as we reasoned that (1) it would cause activation of ERK signaling and dedifferentiation of all SCs distal to the wound, which might provide a pool of proliferating $Nf1^{-/-}$ SCs from which a tumor could develop; and (2) it would trigger a potent inflammatory response along the length of the nerve and might thus provide a protumorigenic environment. We therefore performed partial transections of the right sciatic nerve 15 days following Tmx treatment in both *P0-*$Nf1^{fl/fl}$ and *P0-*$Nf1^{fl/-}$ mice and the corresponding $Nf1^{fl/fl}$ and $Nf1^{fl/-}$ controls. Six to 8 months following injury, the animals were sacrificed and analyzed for changes to the structure of the nerves and tumor formation (Figure 3A). Upon gross dissection, similar high proportions of both *P0-*$Nf1^{fl/fl}$ and *P0-*$Nf1^{fl/-}$ mice exhibited visible tumors at the injury site (33.3% and 34.6%, respectively), indicating that *Nf1* loss in mSCs is able to cooperate with a wounding response to induce tumor formation. These results also showed that the *Nf1* genetic background did not contribute to the rate of tumor formation in this mouse model (Figures 3B and 3C). In contrast, the control animals displayed apparently well-regenerated sciatic nerves. A single exception was one $Nf1^{fl/-}$ mouse, which had a microscopically enlarged nerve. Given the rarity of this event and the fact that it occurred in a heterozygous background, it is tempting to speculate that this tumor may have resulted from loss of heterozygosity at the *Nf1* locus. The unwounded contralateral nerves of the *Nf1* mutants were also unaffected in that they were indistinguishable from uncut controls, arguing against a possible systemic contribution to tumor formation.

The structure and composition of the tumors that developed in *Nf1*-deficient mice were characterized and compared with the equivalent region of control animals at 8 months following injury. Cross-sections of the nerve showed a remarkable enlargement of the peripheral nerves in *Nf1*-deficient mice compared with controls (Figures 3C and S2A), with Hoechst staining showing an increase in cell density in the mutant nerves (Figure S2B). Histological examination of the sciatic nerves by our pathologist revealed that the tumors that developed in the mutant mice could be classified as GEM grade I neurofibromas (Stemmer-Rachamimov et al., 2004). Hematoxylin and eosin (H&E) staining showed that the tumors were composed of increased numbers of disorganized spindle-shaped cells, infiltrating mast cells,

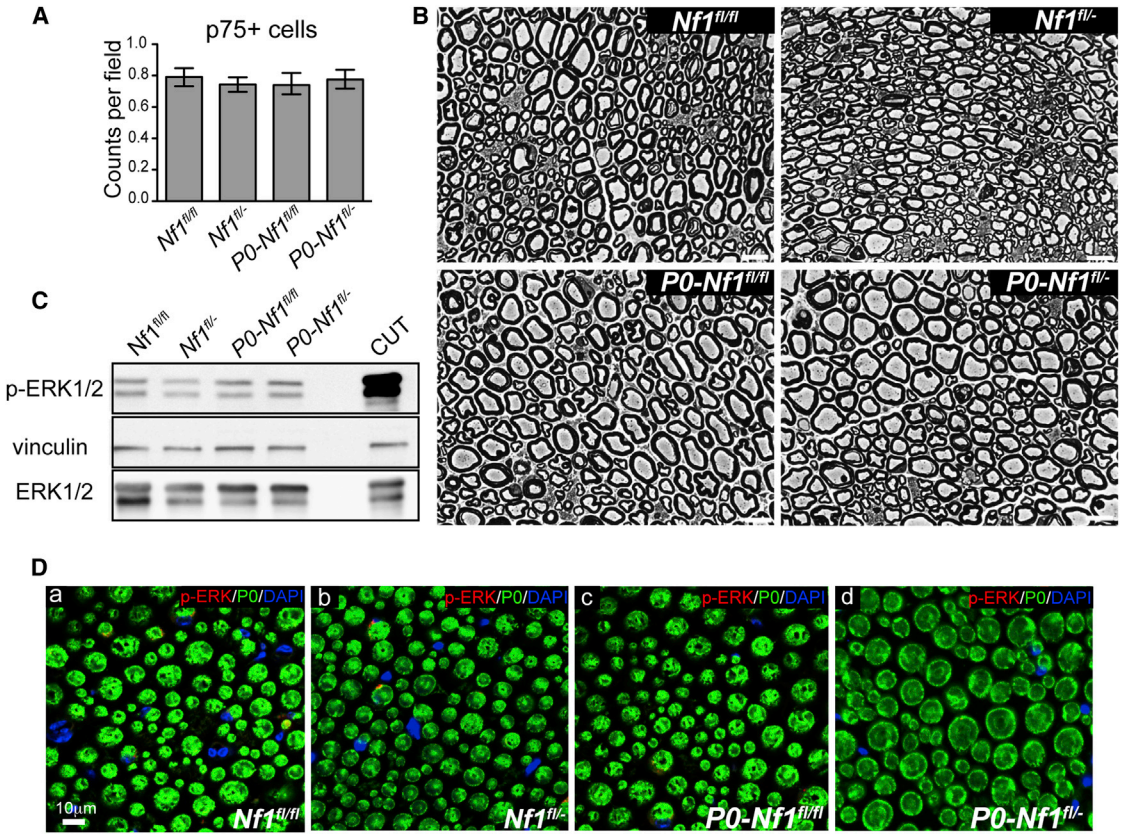

Figure 2. *Nf1* Loss in mSCs Does Not Alter the Sciatic Nerve

(A) Fifteen days after the first Tmx dose, 5- to 6-week-old *P0-Nf1*$^{fl/fl}$ and *P0-Nf1*$^{fl/-}$ mutants and *Nf1*$^{fl/fl}$ and *Nf1*$^{fl/-}$ control mice were treated with Tmx and their sciatic nerves were harvested for analysis. Nerves were processed for immunostaining with p75 antibody to label nonmyelinating/dedifferentiated SCs. The graph shows quantification of p75+ cells per field of view (n = 3 animals for each group; eight fields were counted per section, with three sections per animal; data are represented as mean values ± SEM).

(B) Representative phase-contrast images of toluidine-blue-stained, semithin cross-sections of sciatic nerves from controls (upper panels) and *Nf1* mutants (lower panels) 8 months after Tmx administration. Scale bar is 10 μm.

(C) Western blot analysis of sciatic nerve extracts 15 days after induction of *Nf1* loss shows no alteration of p-ERK levels upon *Nf1* loss (third and fourth lanes). On the right, nerve extracts from control mice 24 hr after nerve transection are shown as a control for ERK activation.

(D) Representative images of cross-sections of sciatic nerves immunostained for p-ERK (red) and P0 (green; n = 3 for each group).

See also Figure S1.

and other inflammatory cells in a collagen-rich matrix, and resembled neurofibromas seen in other GEM models of neurofibroma formation (Figure 3D; Cichowski et al., 1999; Le et al., 2011; Wu et al., 2008; Zheng et al., 2008). Moreover, the tumors were also positive for S100, although the levels were lower than those found within the uninjured part of the nerve (Figures S2C and S2D). Early examination of nerves at 3 months showed that the mutant nerves had small tumors that continued to grow and eventually gave rise to the larger tumors seen at 6–8 months. In addition, a proportion of these tumors (~10%) progressed along the distal stump of the nerve, consistent with the neoplastic nature of these tumors (Figure S2E). EdU-labeling experiments showed increased proliferation rates within the tumor regions compared with those seen in regenerated control nerves, and some of these proliferating cells were SCs (Figures S3A–S3C). Structural analysis of semithin and ultrathin sections confirmed the differences in structure between the regenerated control nerves and the tumors that formed in the *Nf1* mutant mice. Repaired sciatic nerves from control mice were tightly packed with myelinating axons, with little intervening space, and electron microscopy (EM) analysis showed well-organized minifascicles, which form as part of the regeneration process (Figure S3D). There were also no discernible repair abnormalities in the *Nf1*$^{+/-}$ mice, which although previously reported to exhibit skin wound-repair defects (Atit et al., 1999), appeared able to repair nerves normally. In contrast, the tumors in the *Nf1* mutants resembled neurofibromas seen in other mouse models (Cichowski et al., 1999; Wu et al., 2008). They had a highly disorganized structure with a significantly expanded interstitial compartment with increased cellularity between myelinated axons. EM analysis revealed numerous denervated SCs, fibroblasts, "perineurial-like" cells, mast cells, and the occasional "naked" axon in a dense collagen matrix (Figures 3E, 3F, and S3D). Consistent with the mixed-cell

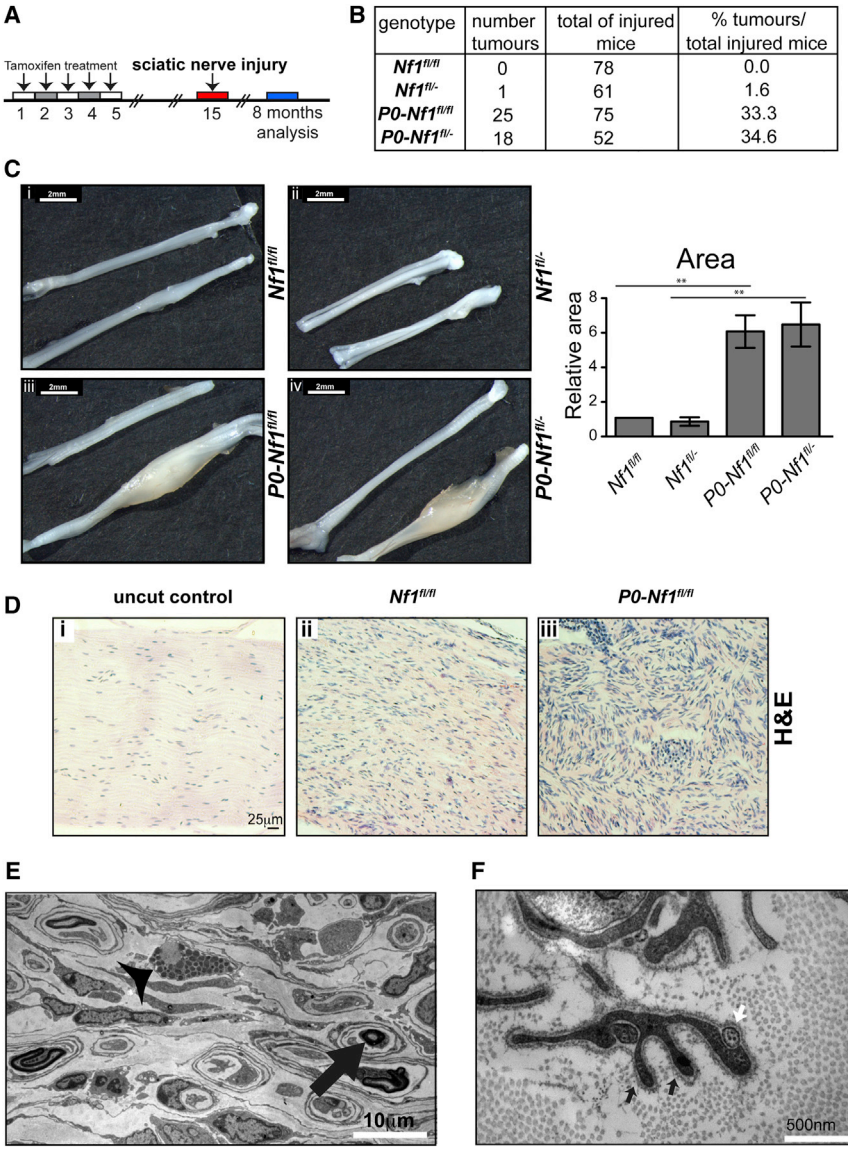

Figure 3. *Nf1* Mutant Mice Form Tumors at the Site of Injury

(A) Schematic representation of the protocol used to assess the effect of injury.

(B) Table shows the frequency of tumor development in the four genotypes studied.

(C) Micrographs show sciatic nerves (uninjured nerves [top panels]) and injured nerves [bottom panels] of age-matched controls (i and ii) and NF1 mutants (iii and iv) Tmx-treated animals, 8 months following injury. Quantification of the size of the tumors, calculated from sections of the tumors, shows mean relative area ± SEM (n = 3 for each genotype).

(D) Control and NF1 mutant mice were sectioned longitudinally and stained with H&E. i: uncut control; ii: control nerve $Nf1^{fl/fl}$ 8 months after injury shows fairly well aligned nuclei, features that are consistent with regeneration. iii: NF1 mutants developed neurofibromas at the injury site. Note the disordered, convoluted bundles of cells exhibiting spindle-cell morphology with ovoid and spindle-shaped nuclei, features that contrast with the regenerative appearance of the cells in ii.

(E) Representative EM image of a $P0\text{-}Nf1^{fl/fl}$ tumor shows a mixture of intact mSCs (arrow), dissociated SCs, "perineurial-like" cells, and mast cells (arrowhead).

(F) Representative image of an SC, identified by a continuous basal lamina (black arrows), found within a $P0\text{-}Nf1^{fl/fl}$ tumor. The white arrow points to a naked axon; abundant collagen deposits are also observed.

See also Figures S2, S3, and S4.

composition of these tumors, immunostaining showed a large increase in the numbers of mast cells, macrophages, neutrophils, and T cells within the tumors compared with the regenerated regions of the control nerves, and activated fibroblasts were found in the tumors but never in the regenerated nerves (Figure S4).

Nf1-Deficient Cells in the Tumor Are Frequently S100− and Can Resemble Perineurial Cells

To define the contribution of *Nf1*-deficient cells in the neurofibromas formed at the injury site, we took advantage of a floxed YFP reporter and crossed it to the $P0\text{-}Nf1^{fl/fl}$ and $P0\text{-}Nf1^{fl/-}$ mutants. Tumors were dissected from these animals 6 months following injury and processed for immunostaining. YFP analysis showed a near uniform distribution of *Nf1*-deficient cells throughout most tumor sections. The majority of the cells were YFP+ and most appeared to be dissociated from axons (Figure 4A). Moreover, the YFP+ cells expressed p75, a marker of dedifferentiated/non-mSCs (Figure 4B), thus clearly demonstrating that loss of *Nf1* in mSCs in the context of a wound results in the maintenance of these cells in their "progenitor-like' state, dissociation from axons, and abnormal proliferation. Indeed, in some tumors, this abnormal behavior included invasion of YFP+ cells into adjacent muscle (Figure 4A).

The ability to "mark" the cells derived from recombined mSCs enabled us to make several observations concerning the "neoplastic" cells within the tumors with relevance to the pathology of the tumors. The first observation was that, although expression of the SC marker S100 is commonly used as a diagnostic criterion of neurofibromas, we found that the YFP+ cells within the tumor were mostly negative for S100. Instead, S100 expression was mostly restricted to intact mSCs, both scattered throughout the tumor and associated with the unwounded regions (Figure 4C). These results were consistent with the low levels of S100 staining seen in paraffin-embedded tumors, which showed low levels of S100+ cells within the tumor but high levels within the undamaged part of the nerve (Figure S2C).

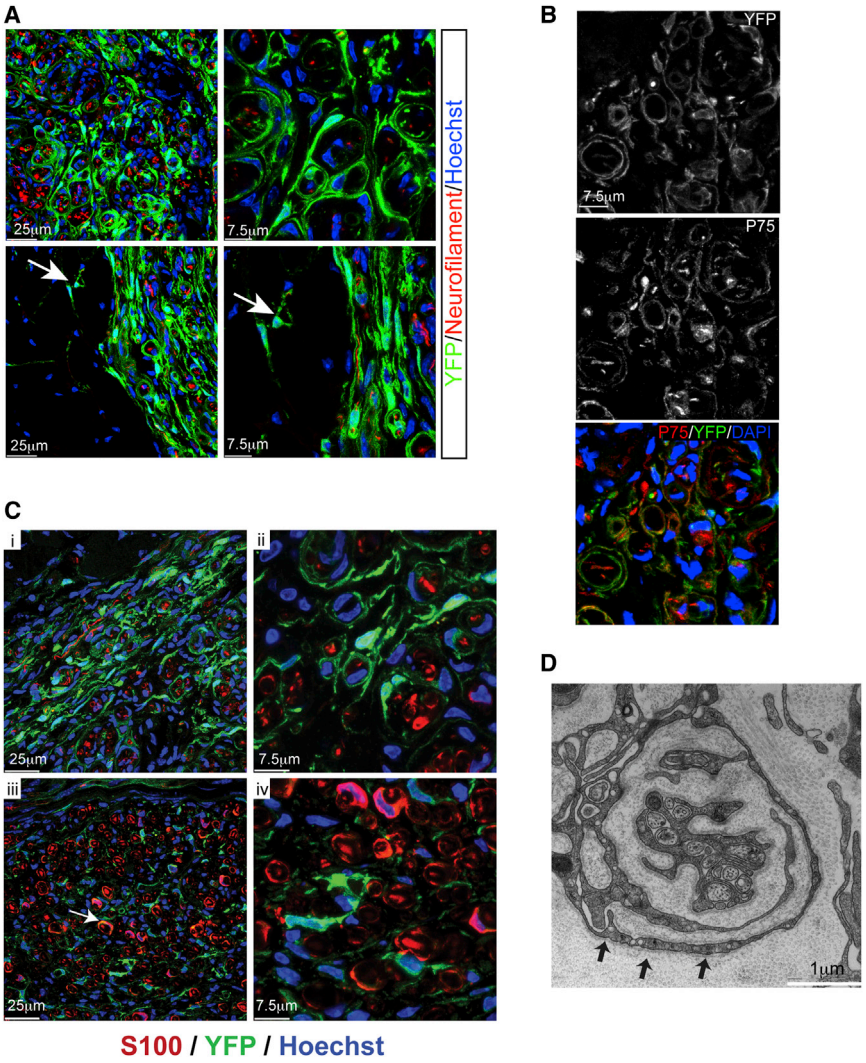

Figure 4. In the Neurofibromas, the Majority of Cells Derive from *Nf1*$^{-/-}$ mSCs and Are S100− and p75+

(A) Representative cross-sections of a neurofibroma dissected from a P0:YFP-Nf1$^{fl/fl}$ animal 6 months after Tmx treatment and nerve wounding, and immunolabeled for neurofilament (red) and YFP (green). Note that the YFP+ cells are devoid of axonal contact and arrows point to YFP+ cells invading the adjacent muscle tissue.

(B) Immunofluorescence of cross-sections of a neurofibroma showing colocalization between YFP (staining *Nf1*$^{-/-}$ SCs) and p75 (dedifferentiated/nonmyelinating SCs). Note that nearly all of the YFP+ cells are positive for p75.

(C) Neurofibroma cryosections from a P0-YFP-*Nf1*$^{fl/fl}$ mouse were immunolabeled for YFP (green) and S100 (red), with nuclei counterstained with Hoechst (blue). Panels i and ii are representative images of the neoplastic region and show that the majority of the YFP+ cells are S100−. Panels iii and iv were taken from the "regenerated area" and show that the majority of cells are S100+. The white arrow points to a YFP+/S100+ cell.

(D) Representative EM image of a perineurial-like cell in a tumor from a *P0-Nf1*$^{fl/fl}$ animal. Arrows point to patchy basal lamina and intracellular vesicles that are characteristic of these cells.

See also Figure S5.

The second observation was that some of the YFP+ cells within the tumor exhibited the morphology traditionally attributed to "perineurial-like" cells, which commonly make up a high proportion of neurofibromas (Figures 4B and S5B; Erlandson, 1985). These extremely thin cells exhibit long cytoplasmic processes enwrapping other cells and could be seen in all the tumors, albeit at varying frequency both between and within the tumors (compare the upper and lower panels of Figure 4A), which is consistent with a study of human neurofibromas (Lassmann et al., 1976). A comparison of immunofluorescence images and EM micrographs revealed a striking resemblance between many of the YFP/p75-expressing cells and cells that are frequently found in EM images of neurofibromas and traditionally are identified as "perineurial-like" (Figures S5A and S5B; Erlandson, 1991). Moreover, ultrastructural analysis showed that these cells contained multiple pinocytic vesicles and a partial basement membrane that is characteristic of these cells (Figures 4D and S5A). This suggests that despite their distinct ultrastructural morphology, many of these cells are derived from mSCs and contribute to the neoplastic potential of the tumor. To characterize these cells further, we used two markers of perineurial cells, Glut1 and epithelial membrane antigen (EMA). In control nerves, we were able to show that Glut1 specifically stained the perineurial cells and the blood vessels (Figure S5B); however, consistent with other studies, we could not detect any EMA+ cells within the mouse nerve (Takebe et al., 2008). In contrast, within the tumors we detected multiple Glut1+ cells. Consistent with the observation that some of the YFP+ cells resembled perineurial cells, a proportion of the YFP+ cells with a perineurial-like morphology were positive for Glut1 (Figure S4D). However, only a proportion of these perineurial-like cells were YFP+, which suggests that "normal" perineurial cells, or possibly pericytes, are also behaving abnormally and make up a significant component of the tumor. Finally, we were able to identify rare YFP+ cells that were negative for both S100 and p75 markers, suggesting that neurofibromas may contain rare cell populations derived from P0+ mSCs that have lost their original identity (Figure S5B). In contrast to the homogeneous distribution of YFP+ cells in neurofibromas, only a few positive cells were found at the injury site in controls (Figure S5E).

Distal to the Wound Site, *Nf1*-Deficient SCs Remyelinate Normally

An important observation was that tumors only develop at the wound site. After nerve injury, strong Ras-Raf-ERK activation

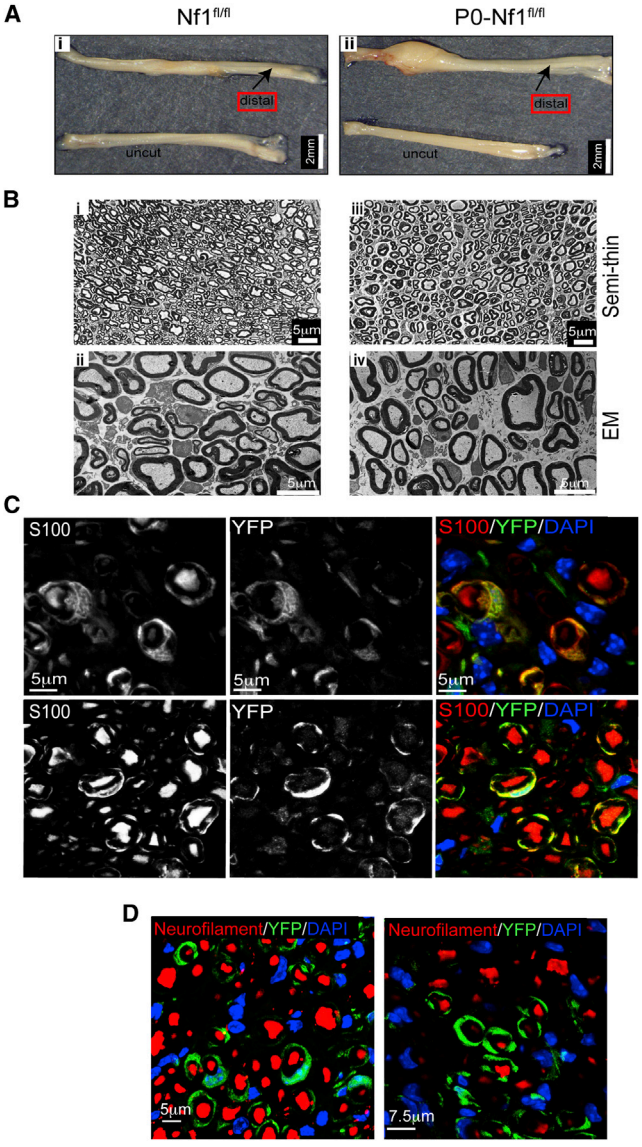

Figure 5. Distal to the Wound Site, *Nf1*$^{-/-}$ SCs Redifferentiate and Nerves Regenerate Normally

(A) Photographs showing the injured and the contralateral uninjured nerves of control (i) and *Nf1* mutant (ii) mice 8 months following Tmx treatment and nerve partial transection.

(B) Representative phase-contrast images of semithin sections stained with toluidine blue (i and iii) and EM images (ii and iv) of control (left) and *NF1*$^{fl/fl}$ (right) mice.

(C) Sections were prepared from the nerve region distal to the neurofibromas formed in *Nf1* mutants (upper panel) and the equivalent region of control wounded nerves (lower panel) and immunolabeled for S100 (red) and YFP (green).

(D) YFP+*Nf1*$^{-/-}$ SCs are found associated with large caliber axons (immunostained for neurofilament in red) 6 months following Tmx treatment and partial nerve transection.

See also Figure S4.

followed by dedifferentiation and proliferation is seen in all SCs at the wound site and throughout the entire distal stump. Moreover, there is a robust inflammatory response throughout the length of the distal stump. To determine the structure of the regenerated nerves in the control and mutant nerves, we performed a structural analysis, which showed that distal to the injury, control and mutant mice nerves regenerated to a similar extent and were indistinguishable (Figures 5A and 5B). These results indicated that, in contrast to the wound site, in the environment of the distal nerve stump, *Nf1*$^{-/-}$ SCs appeared to behave normally. However, as we only achieved a maximum of 50% recombination, a separate possibility was that *Nf1*$^{-/-}$ SCs failed to reassociate with the regenerating axons and as a result died or were otherwise lost from the nerve. To exclude this possibility, we examined the fate of *Nf1*$^{-/-}$ SCs (YFP+) in the distal region of mutant mice in which tumors had developed at the wound site. In sharp contrast to what we encountered at the tumor site, we found that nearly all YFP+ cells were associated with axons and expressed S100 (Figures 5C and 5D). Many were myelinating, indicating they had returned to their original fate; however, the occasional YFP+ cell was found to be p75+ and associated with axons, suggesting that *Nf1*$^{-/-}$ mSCs were capable of differentiating to the nonmyelinating cell type following an injury. These results demonstrate that an identical genetic insult to a specific target cell can have distinct outcomes depending on the microenvironmental context. In the distal stump of the nerve, the environment is tumor suppressive, with dedifferentiated SCs reassociating with regrowing axons and undergoing redifferentiation. In contrast, at the wound site the environment is tumor promoting. However, consistent with a role for the ERK signaling pathway in maintaining the dedifferentiated state and driving SC proliferation, sustained elevated levels of ERK signaling were detected specifically at the wound site in the *Nf1* mutant animals. Western blot analysis showed that in contrast to control animals, in which P-ERK levels returned to low levels by day 5 after injury, the P-ERK levels remained high in the mutant nerves (Figure 6A). Moreover, immunostaining showed that the elevated signaling was confined to the injury site from which the tumor developed, and was associated with increased proliferation of *Nf1*$^{-/-}$ cells specifically at the wound site (Figures 6B and 6C).

DISCUSSION

Identifying the "cell of origin" from which tumors can or do derive has been the aim of many recent animal models of cancer. The results have been diverse, with cancers shown to be capable of arising from stem cell and progenitor populations but also sometimes from fully differentiated cell types (Visvader, 2011). In NF1-associated neurofibromas, the picture is similarly complex. A series of mouse models in which *Nf1* was specifically deleted from the SC lineage at various developmental stages indicated that for tumors to occur, *Nf1* had to be lost during a specific developmental window at approximately embryonic day 13 (Joseph et al., 2008; Wu et al., 2008; Zheng et al., 2008). However, the tumors only developed later in adulthood and appeared to derive from the nonmyelinating population. In contrast, in a separate study, transplant experiments suggested that dermal neurofibromas could derive from neural-crest-like stem cells termed skin-derived precursors (SKPs) (Le et al., 2009). In this study, we used a highly specific promoter to delete *Nf1* from mSCs in adult mice to determine whether these highly

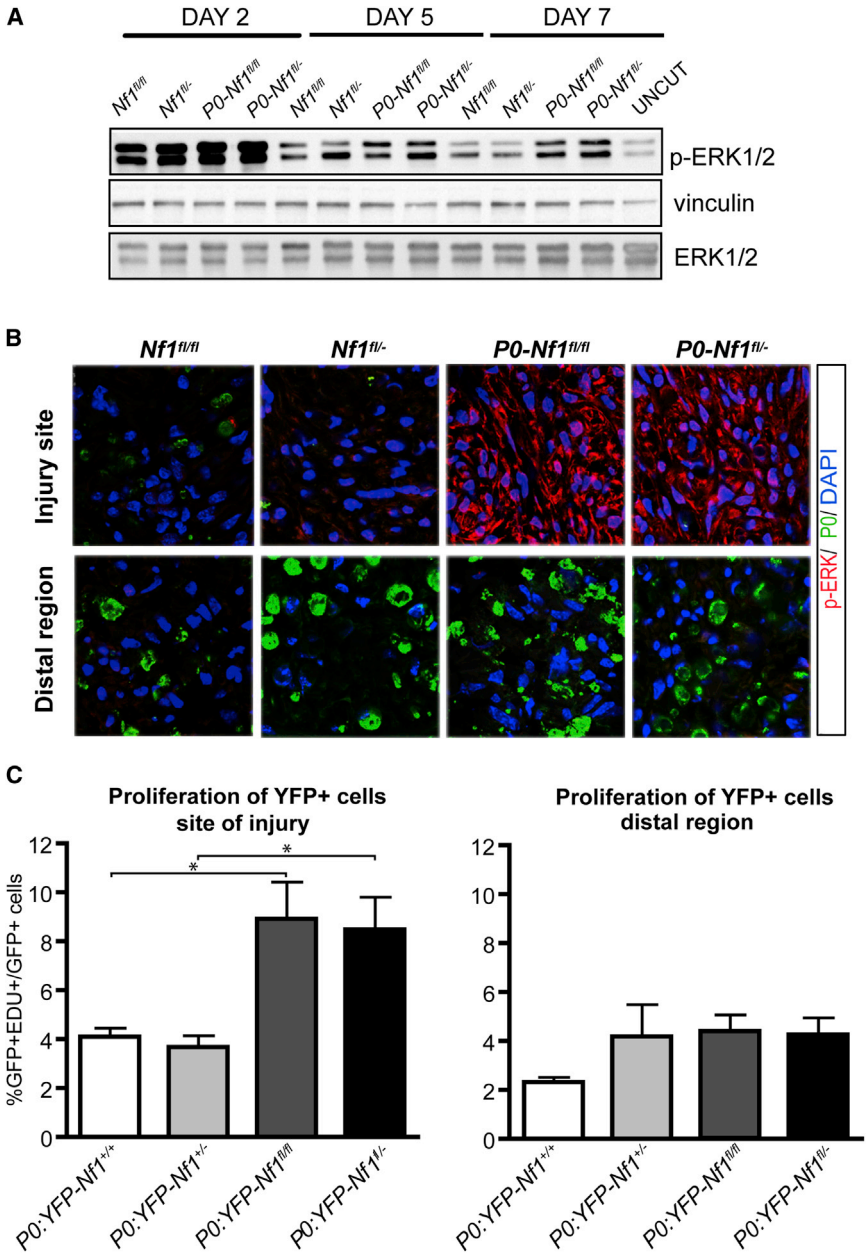

Figure 6. ERK Signaling Is Deregulated in Sciatic Nerves of *Nf1*-Deficient Mice following Injury

(A) Western blot analysis of sciatic nerves from control ($Nf1^{fl/fl}$ and $Nf1^{fl/-}$) and *Nf1* mutant ($P0\text{-}Nf1^{fl/fl}$ and $P0\text{-}Nf1^{fl/-}$) mice at the indicated time points after injury. Note that the ERK signal is sustained at day 7 in mutant mice (blot representative of four different animals for each genotype).

(B) Seven days after injury, cryosections of sciatic nerves were immunolabeled for the mSC marker P0 (green) and p-ERK (red). Nuclei were counterstained with DAPI. Upper panel: site of injury; bottom panel: distal region. ERK pathway activation is sustained only at the site of injury in *Nf1* mutants (representative images of three animals analyzed for each group).

(C) EdU incorporation was assessed 7 days after injury in control and mutant mice at the site of injury (left) and distal to the injury site (right). Results show the means of EdU+/YFP+ cells ± SEM (n = 3 of each group); *p < 0.05.

specialized, quiescent cells can give rise to neurofibromas. We found that, alone, loss of *Nf1* in mSCs had no effect on nerve structure and did not result in tumor formation. However, neurofibromas formed with high efficiency following damage to the *Nf1*-depleted nerve. Although these results do not address whether tumors can derive from adult non-mSCs, they clearly demonstrate that adult mSCs can be the "cell of origin" for neurofibromas, and that cooperating microenvironmental signals found only at the wound site are essential for tumors to form.

The finding that tumors only develop at the wound site has several important implications. Following a nerve injury, mSCs dedifferentiate along the length of the nerve in response to a sustained signal through the ERK signaling pathway and there is a robust inflammatory response along the length of the nerve. The fact that tumors only form at the injury site shows that robust activation of ERK signaling, dedifferentiation and proliferation of SCs, and an inflammatory response is not sufficient to trigger tumor formation but that tumor formation also requires the specific microenvironment of the wound site. While an important question that remains to be resolved involves the nature of these cooperating signals at the wound site, an equally important question is, why do $Nf1^{-/-}$ SCs behave normally within the distal stump of the nerve, acting as wild-type cells to remyelinate the regrown axons? The "tumor-suppressive" environment of the nerve is further indicated by the earlier studies in which *Nf1* was deleted from SCs during embryogenesis. In these studies, the $Nf1^{-/-}$ SCs behaved more or less normally to form both Remak Bundles and myelinated axons (Wu et al., 2008; Zheng et al., 2008). It was only during adulthood that slight defects in the Remak bundles could be observed, and it was suggested that tumors derived from these destabilized structures. Although these studies suggested that tumors derive from adult non-mSCs, their models are somewhat similar to ours in that the destabilization of the Remak bundles resembles aspects of the injured state artificially induced in our model. Consistent with this idea, tumor formation was associated with an early inflammatory response. It is possible that tumors developed from the nonmyelinating population because loss of *Nf1* at that specific developmental stage specifically affected the stability of Remak bundles, and that tumors could also develop from mSCs in these mice if they were injured. The finding that loss of

Nf1 in adult SCs does not result in efficient tumor formation is also consistent with a separate study in which *Nf1* was deleted in adult SCs and tumors only arose in rare cases in older animals (Le et al., 2011). It is not an unlikely scenario that tumors arose in these animals following a naturally occurring traumatic injury.

The tumor-suppressive environment of the nerve is further highlighted by observations that in vitro, *Nf1* loss in SCs is sufficient to induce a Ras-like phenotype and elevated Ras/Raf/ERK signaling that inhibits SC–axonal interactions and blocks SC differentiation, indicating that neurofibromin is a limiting GAP in the in vitro environment (Napoli et al., 2012; Parrinello et al., 2008). This must mean that within the nerve, either neurofibromin is not a limiting GAP or the environment can act to suppress the ERK signaling pathway. Moreover, it might also suggest that the tumor-promoting wound environment mimics the in vitro environment, which is consistent with the view that in vitro culture reflects an in vivo wounded response (Iyer et al., 1999). It will be crucial to dissect the mechanisms involved, as identification of both tumor-suppressive and tumor-promoting signals will lead to useful therapeutic targets that could potentially prevent the development of tumors both during development and in adulthood.

A link between wounding and tumorigenesis has long been recognized (Balkwill and Mantovani, 2001; Martins-Green et al., 1994). Recent mouse models in the pancreas and skin have shown that an injured or chronically inflamed environment is a critical cooperating event with specific genetic changes in order for tumors to occur, and these models have parallels to human diseases in which chronic tissue damage can precede tumor formation (Arwert et al., 2012; Guerra et al., 2007; Kasper et al., 2011; Wong and Reiter, 2011). Importantly, there is a long-standing clinical hypothesis that neurofibroma formation is fostered by local trauma and injury, and hence neurofibromas are often referred to as unrepaired wounds. Our results are consistent with this hypothesis and indeed suggest that a neurofibroma could be considered as an "exaggerated or neoplastic neuroma"—an unrepaired "wound" of the peripheral nerve (Lassmann et al., 1976; Riccardi, 1992, 2007). Because NF1 patients are born heterozygous for *NF1*, with the loss of the second allele, a bottleneck event for neurofibroma formation, injury is likely to increase the frequency of this event by inducing SC proliferation. Importantly, however, our results indicate that injury may play an additional role by creating a protumorigenic microenvironment required by *NF1*-deficient cells to induce tumorigenesis. To determine whether this is the case, it will be important to define the nature of the protumorigenic environment, establish whether it is induced by the more common types of human nerve injuries (e.g., crush injuries), and determine a link to tumorigenesis in patients with such injuries.

A fascinating observation in a previous model of NF1 is that tumors only develop in a $Nf1^{+/-}$ background, implicating other $Nf1^{+/-}$ cell types, in particular mast cells, in neurofibroma formation (Yang et al., 2008; Zhu et al., 2002). In contrast, we found that the *Nf1* background had no effect on the rate of tumor formation, given that tumors formed with similar efficiencies in both $Nf1^{+/+}$ and $Nf1^{+/-}$ mice. The mechanism proposed by the previous studies is that mast cells cooperate with $Nf1^{-/-}$ SCs to form tumors, and that $Nf1^{+/-}$ mast cells are more efficiently attracted to signals from $Nf1^{-/-}$ SCs (Yang et al., 2003). One possible explanation for the discrepancy with our results is that the wound site attracts sufficient wild-type mast cells and that these cells are capable of cooperating in tumor formation. It will be important to test this theory in a mast-cell-negative mouse.

The ability to track the $Nf1^{-/-}$ cells derived from mSCs permitted us to make observations that may have important clinical implications. $Nf1^{-/-}$ mSC-derived cells were a major component of the tumors that developed at the injury site. Surprisingly, however, we observed that the majority of the YFP+ $Nf1^{-/-}$ mSC-derived cells within the tumor region were negative for the SC marker S100, which is commonly used to diagnose these tumors. Instead, the S100+ cells within the tumor were mostly YFP− and appeared to be the result of normal SCs within the tumors, as they appeared to be interacting mostly with axons. This is reminiscent of previous observations made by Cichowski et al. (1999) in neurofibromas in a $Nf1^{+/-}$;$Nf1^{-/-}$ chimeric mouse model, and may be consistent with the often low levels of S100 seen in human tumors (Hirose et al., 2003; Tucker et al., 2011). Importantly, the analysis of YFP+/S100−/p75+ cells also revealed that a number of these mSC-derived cells appeared to be morphologically distinct from SCs. Instead, they exhibited a characteristic morphology (a long cytoplasmic process displayed in arrays or enwrapping other cells) associated with "perineurial-like" cells, which are a frequent cellular component of neurofibromas and are often considered to be of fibroblast origin. However, it was previously speculated based on ultrastructural studies that these cells could derive from SCs, as frequent "transitional" cells with shared SC/perineurial features were observed (Erlandson, 1991). Our results indicate that some of these cells most likely originate from $NF1^{-/-}$ SCs and are likely to be key drivers of the tumor.

In summary, our results demonstrate that neurofibromas can originate from adult mSCs following loss of *Nf1*. However, tumor formation requires a protumorigenic environment that can be provided by signals specifically found at the site of a nerve injury. In contrast, these results indicate that, normal nerves constitute a tumor-suppressive environment. This mouse model gave us the opportunity to track the fate of $Nf1^{-/-}$-induced mSCs, which led to the important observation that these cells give rise to both S100− tumor cells and tumor cells with a "perineurial-like" morphology. In future studies, investigators will be able to track the initial development of these tumors and identify mechanisms by which environmental signals can contribute to tumor formation.

EXPERIMENTAL PROCEDURES

Mouse Strains

$Nf1^{flox/flox}$ (Zhu et al., 2001) and $Nf1^{flox/-}$ (Jacks et al., 1994) on a mixed 129/Bl/6 background were crossed with *P0CreERT2* C57Bl/6 mice (Leone et al., 2003) to generate *P0-Nf1*$^{fl/fl}$ and *P0-Nf1*$^{fl/-}$ mice. *P0-Nf1*$^{fl/fl}$ and *P0-Nf1*$^{fl/-}$ mice were bred to LacZRosa (Soriano, 1999) and to YFPRosa (Soriano, 1999).

Tmx Treatment and Nerve Partial Transections

Tmx (Sigma) was dissolved in sunflower oil at 20 mg/ml and filtered through a 0.2 μm filter. Control and *Nf1* mutant mice (5–6 weeks old) received intraperitoneal injections of 2 mg of Tmx once a day for 5 consecutive days. Fifteen days after the first Tmx injection, the mice were anesthetized with isoflurane and the right sciatic nerve was exposed at the sciatic notch. The nerve was half-transected using scissors, so that the perineurium was breeched and

approximately half of the axons were severed within each nerve. The wound was then closed with clips. The entire nerve and the unwounded contralateral were recovered at the indicated time points following surgery. Nerves were immediately fixed in 4% paraformaldehyde for immunohistochemistry or frozen in liquid nitrogen for protein analysis.

Cell Proliferation Assay

Cell proliferation was measured by EdU incorporation (Invitrogen). Mice were pulsed with 1 mg of EdU at 5 hr before sacrifice. The sciatic nerves were dissected and processed for immunofluorescence. Nerve sections were then stained using the Click-iT EdU cell proliferation assay kit (Invitrogen) according to the manufacturer's instructions.

Statistical Analysis

The data are represented as mean values ± SEM. One-way ANOVA with Bonferroni post hoc test was used for statistical analysis, and p values considered significant were indicated by asterisks as follows: *$p < 0.05$, **$p < 0.01$, and ***$p < 0.001$.

For further details regarding the materials and methods used in this work, please see the Extended Experimental Procedures.

SUPPLEMENTAL INFORMATION

Supplemental Information includes Extended Experimental Procedures and five figures and can be found with this article online at http://dx.doi.org/10.1016/j.celrep.2013.08.033.

ACKNOWLEDGMENTS

We thank the reviewers for their useful comments regarding the manuscript. This work was supported by a grant from the Association for International Cancer Research and a program grant from Cancer Research UK. S.R. was funded by the GABBA Graduate Program and was supported by grant SFRH/BD/33254/2007 from Fundação da Ciência e Tecnologia. I.N. was partly supported by an EMBO fellowship. U.S. is supported by the Swiss National Science Foundation. A.M.F. was supported by the National Institute for Health Research, UCLH Biomedical Centre, and UCL Experimental Cancer Centre.

Received: March 5, 2013
Revised: July 23, 2013
Accepted: August 20, 2013
Published: September 26, 2013

REFERENCES

Arwert, E.N., Hoste, E., and Watt, F.M. (2012). Epithelial stem cells, wound healing and cancer. Nat. Rev. Cancer *12*, 170–180.

Atit, R.P., Crowe, M.J., Greenhalgh, D.G., Wenstrup, R.J., and Ratner, N. (1999). The Nf1 tumor suppressor regulates mouse skin wound healing, fibroblast proliferation, and collagen deposited by fibroblasts. J. Invest. Dermatol. *112*, 835–842.

Balkwill, F., and Mantovani, A. (2001). Inflammation and cancer: back to Virchow? Lancet *357*, 539–545.

Basu, T.N., Gutmann, D.H., Fletcher, J.A., Glover, T.W., Collins, F.S., and Downward, J. (1992). Aberrant regulation of ras proteins in malignant tumour cells from type 1 neurofibromatosis patients. Nature *356*, 713–715.

Brannan, C.I., Perkins, A.S., Vogel, K.S., Ratner, N., Nordlund, M.L., Reid, S.W., Buchberg, A.M., Jenkins, N.A., Parada, L.F., and Copeland, N.G. (1994). Targeted disruption of the neurofibromatosis type-1 gene leads to developmental abnormalities in heart and various neural crest-derived tissues. Genes Dev. *8*, 1019–1029.

Cichowski, K., Shih, T.S., Schmitt, E., Santiago, S., Reilly, K., McLaughlin, M.E., Bronson, R.T., and Jacks, T. (1999). Mouse models of tumor development in neurofibromatosis type 1. Science *286*, 2172–2176.

DeClue, J.E., Papageorge, A.G., Fletcher, J.A., Diehl, S.R., Ratner, N., Vass, W.C., and Lowy, D.R. (1992). Abnormal regulation of mammalian p21ras contributes to malignant tumor growth in von Recklinghausen (type 1) neurofibromatosis. Cell *69*, 265–273.

Erlandson, R.A. (1985). Peripheral nerve sheath tumors. Ultrastruct. Pathol. *9*, 113–122.

Erlandson, R.A. (1991). The enigmatic perineurial cell and its participation in tumors and in tumorlike entities. Ultrastruct. Pathol. *15*, 335–351.

Fawcett, J.W., and Keynes, R.J. (1990). Peripheral nerve regeneration. Annu. Rev. Neurosci. *13*, 43–60.

Ferner, R.E. (2007). Neurofibromatosis 1 and neurofibromatosis 2: a twenty first century perspective. Lancet Neurol. *6*, 340–351.

Guerra, C., Schuhmacher, A.J., Cañamero, M., Grippo, P.J., Verdaguer, L., Pérez-Gallego, L., Dubus, P., Sandgren, E.P., and Barbacid, M. (2007). Chronic pancreatitis is essential for induction of pancreatic ductal adenocarcinoma by K-Ras oncogenes in adult mice. Cancer Cell *11*, 291–302.

Hirose, T., Tani, T., Shimada, T., Ishizawa, K., Shimada, S., and Sano, T. (2003). Immunohistochemical demonstration of EMA/Glut1-positive perineurial cells and CD34-positive fibroblastic cells in peripheral nerve sheath tumors. Mod. Pathol. *16*, 293–298.

Iyer, V.R., Eisen, M.B., Ross, D.T., Schuler, G., Moore, T., Lee, J.C., Trent, J.M., Staudt, L.M., Hudson, J., Jr., Boguski, M.S., et al. (1999). The transcriptional program in the response of human fibroblasts to serum. Science *283*, 83–87.

Jacks, T., Shih, T.S., Schmitt, E.M., Bronson, R.T., Bernards, A., and Weinberg, R.A. (1994). Tumour predisposition in mice heterozygous for a targeted mutation in Nf1. Nat. Genet. *7*, 353–361.

Jessen, K.R., and Mirsky, R. (2005). The origin and development of glial cells in peripheral nerves. Nat. Rev. Neurosci. *6*, 671–682.

Joseph, N.M., Mosher, J.T., Buchstaller, J., Snider, P., McKeever, P.E., Lim, M., Conway, S.J., Parada, L.F., Zhu, Y., and Morrison, S.J. (2008). The loss of Nf1 transiently promotes self-renewal but not tumorigenesis by neural crest stem cells. Cancer Cell *13*, 129–140.

Kasper, M., Jaks, V., Are, A., Bergström, A., Schwäger, A., Svärd, J., Teglund, S., Barker, N., and Toftgård, R. (2011). Wounding enhances epidermal tumorigenesis by recruiting hair follicle keratinocytes. Proc. Natl. Acad. Sci. USA *108*, 4099–4104.

Kim, H.A., Ling, B., and Ratner, N. (1997). Nf1-deficient mouse Schwann cells are angiogenic and invasive and can be induced to hyperproliferate: reversion of some phenotypes by an inhibitor of farnesyl protein transferase. Mol. Cell. Biol. *17*, 862–872.

Lassmann, H., Jurecka, W., and Gebhart, W. (1976). Some electron microscopic and autoradiographic results concerning cutaneous neurofibromas in von Recklinghausen's disease. Arch. Dermatol. Res. *255*, 69–81.

Le, L.Q., and Parada, L.F. (2007). Tumor microenvironment and neurofibromatosis type I: connecting the GAPs. Oncogene *26*, 4609–4616.

Le, L.Q., Shipman, T., Burns, D.K., and Parada, L.F. (2009). Cell of origin and microenvironment contribution for NF1-associated dermal neurofibromas. Cell Stem Cell *4*, 453–463.

Le, L.Q., Liu, C., Shipman, T., Chen, Z., Suter, U., and Parada, L.F. (2011). Susceptible stages in Schwann cells for NF1-associated plexiform neurofibroma development. Cancer Res. *71*, 4686–4695.

Leone, D.P., Genoud, S., Atanasoski, S., Grausenburger, R., Berger, P., Metzger, D., Macklin, W.B., Chambon, P., and Suter, U. (2003). Tamoxifen-inducible glia-specific Cre mice for somatic mutagenesis in oligodendrocytes and Schwann cells. Mol. Cell. Neurosci. *22*, 430–440.

Martin, G.A., Viskochil, D., Bollag, G., McCabe, P.C., Crosier, W.J., Haubruck, H., Conroy, L., Clark, R., O'Connell, P., Cawthon, R.M., et al. (1990). The GAP-related domain of the neurofibromatosis type 1 gene product interacts with ras p21. Cell *63*, 843–849.

Martins-Green, M., Boudreau, N., and Bissell, M.J. (1994). Inflammation is responsible for the development of wound-induced tumors in chickens infected with Rous sarcoma virus. Cancer Res. *54*, 4334–4341.

Messing, A., Behringer, R.R., Hammang, J.P., Palmiter, R.D., Brinster, R.L., and Lemke, G. (1992). P0 promoter directs expression of reporter and toxin genes to Schwann cells of transgenic mice. Neuron *8*, 507–520.

Messing, A., Behringer, R.R., Wrabetz, L., Hammang, J.P., Lemke, G., Palmiter, R.D., and Brinster, R.L. (1994). Hypomyelinating peripheral neuropathies and schwannomas in transgenic mice expressing SV40 T-antigen. J. Neurosci. *14*, 3533–3539.

Napoli, I., Noon, L.A., Ribeiro, S., Kerai, A.P., Parrinello, S., Rosenberg, L.H., Collins, M.J., Harrisingh, M.C., White, I.J., Woodhoo, A., and Lloyd, A.C. (2012). A central role for the ERK-signaling pathway in controlling Schwann cell plasticity and peripheral nerve regeneration in vivo. Neuron *73*, 729–742.

Parrinello, S., and Lloyd, A.C. (2009). Neurofibroma development in NF1—insights into tumour initiation. Trends Cell Biol. *19*, 395–403.

Parrinello, S., Noon, L.A., Harrisingh, M.C., Wingfield Digby, P., Rosenberg, L.H., Cremona, C.A., Echave, P., Flanagan, A.M., Parada, L.F., and Lloyd, A.C. (2008). NF1 loss disrupts Schwann cell-axonal interactions: a novel role for semaphorin 4F. Genes Dev. *22*, 3335–3348.

Riccardi, V.M. (1992). Neurofibromatosis: Phenotype, Natural History and Pathogenesis, Second Edition (Baltimore, MD: The John Hopkins University Press).

Riccardi, V.M. (2007). The genetic predisposition to and histogenesis of neurofibromas and neurofibrosarcoma in neurofibromatosis type 1. Neurosurg. Focus *22*, E3.

Scherer, S.S., and Salzer, J.L. (2001). Axon-Schwann cell interactions during peripheral nerve degeneration and regeneration. In Glial Cell Development, K.R. Jessen and W.D. Richardson, eds. (Oxford: Oxford University Press).

Soriano, P. (1999). Generalized lacZ expression with the ROSA26 Cre reporter strain. Nat. Genet. *21*, 70–71.

Stemmer-Rachamimov, A.O., Louis, D.N., Nielsen, G.P., Antonescu, C.R., Borowsky, A.D., Bronson, R.T., Burns, D.K., Cervera, P., McLaughlin, M.E., Reifenberger, G., et al. (2004). Comparative pathology of nerve sheath tumors in mouse models and humans. Cancer Res. *64*, 3718–3724.

Takebe, K., Nio-Kobayashi, J., Takahashi-Iwanaga, H., and Iwanaga, T. (2008). Histochemical demonstration of a monocarboxylate transporter in the mouse perineurium with special reference to GLUT1. Biomed. Res. *29*, 297–306.

Tucker, T., Riccardi, V.M., Brown, C., Fee, J., Sutcliffe, M., Vielkind, J., Wechsler, J., Wolkenstein, P., and Friedman, J.M. (2011). S100B and neurofibromin immunostaining and X-inactivation patterns of laser-microdissected cells indicate a multicellular origin of some NF1-associated neurofibromas. J. Neurosci. Res. *89*, 1451–1460.

Visvader, J.E. (2011). Cells of origin in cancer. Nature *469*, 314–322.

Wong, S.Y., and Reiter, J.F. (2011). Wounding mobilizes hair follicle stem cells to form tumors. Proc. Natl. Acad. Sci. USA *108*, 4093–4098.

Wu, J., Williams, J.P., Rizvi, T.A., Kordich, J.J., Witte, D., Meijer, D., Stemmer-Rachamimov, A.O., Cancelas, J.A., and Ratner, N. (2008). Plexiform and dermal neurofibromas and pigmentation are caused by Nf1 loss in desert hedgehog-expressing cells. Cancer Cell *13*, 105–116.

Xu, G.F., Lin, B., Tanaka, K., Dunn, D., Wood, D., Gesteland, R., White, R., Weiss, R., and Tamanoi, F. (1990). The catalytic domain of the neurofibromatosis type 1 gene product stimulates ras GTPase and complements ira mutants of S. cerevisiae. Cell *63*, 835–841.

Yang, F.C., Ingram, D.A., Chen, S., Hingtgen, C.M., Ratner, N., Monk, K.R., Clegg, T., White, H., Mead, L., Wenning, M.J., et al. (2003). Neurofibromin-deficient Schwann cells secrete a potent migratory stimulus for Nf1+/- mast cells. J. Clin. Invest. *112*, 1851–1861.

Yang, F.C., Ingram, D.A., Chen, S., Zhu, Y., Yuan, J., Li, X., Yang, X., Knowles, S., Horn, W., Li, Y., et al. (2008). Nf1-dependent tumors require a microenvironment containing Nf1+/− and c-kit-dependent bone marrow. Cell *135*, 437–448.

Zheng, H., Chang, L., Patel, N., Yang, J., Lowe, L., Burns, D.K., and Zhu, Y. (2008). Induction of abnormal proliferation by nonmyelinating Schwann cells triggers neurofibroma formation. Cancer Cell *13*, 117–128.

Zhu, Y., Romero, M.I., Ghosh, P., Ye, Z., Charnay, P., Rushing, E.J., Marth, J.D., and Parada, L.F. (2001). Ablation of NF1 function in neurons induces abnormal development of cerebral cortex and reactive gliosis in the brain. Genes Dev. *15*, 859–876.

Zhu, Y., Ghosh, P., Charnay, P., Burns, D.K., and Parada, L.F. (2002). Neurofibromas in NF1: Schwann cell origin and role of tumor environment. Science *296*, 920–922.

Zochodne, D.W. (2008). Neurobiology of Peripheral Nerve Regeneration, First Edition (New York: Cambridge University Press).